Biometals (2022) 35:1133–1143
https://doi.org/10.1007/s10534-022-00429-x

$Ca_2Fe_2O_5$ powder antifungal activity to the *Candida utilis* culture upon its growth

Svetlana Vihodceva · Vasily Bankovskis · Olga Muter · Andris Šutka

Received: 1 December 2021 / Accepted: 27 July 2022 / Published online: 15 August 2022

Abstract This study reports the impact of $Ca_2Fe_2O_5$ porous powder on the yeast *Candida utilis*—as a fungal model—at different phases of growth, i.e., early exponential (6 h), mid-log (11 h), and stationary (17 h) phases. $Ca_2Fe_2O_5$ inhibited the cell growth in a time-dependent manner. After 120 min incubation, the fungicidal activity of porous powder was observed, i.e., log reduction of 2.81 and 2.58 for 11 and 17 h cultures, respectively, reaching the maximum of 4 log reduction after 7 days. Nevertheless, the 6 h culture of *C. utilis* showed enhanced resistance to $Ca_2Fe_2O_5$ with a $\leq$0.4 log reduction during the 7 days exposure. Our results not only showed that $Ca_2Fe_2O_5$ has the potential to effectively eliminate the *C. utilis* cell growth but also indicated the importance of the yeast culture physiological state for resistance to $Ca_2Fe_2O_5$. To the best of our knowledge, this is the first study that evaluated the fungicidal activity of $Ca_2Fe_2O_5$ porous powder on *C. utilis* and the impact of the *C. utilis* phase of growth on the cell susceptibility.

Graphical abstract

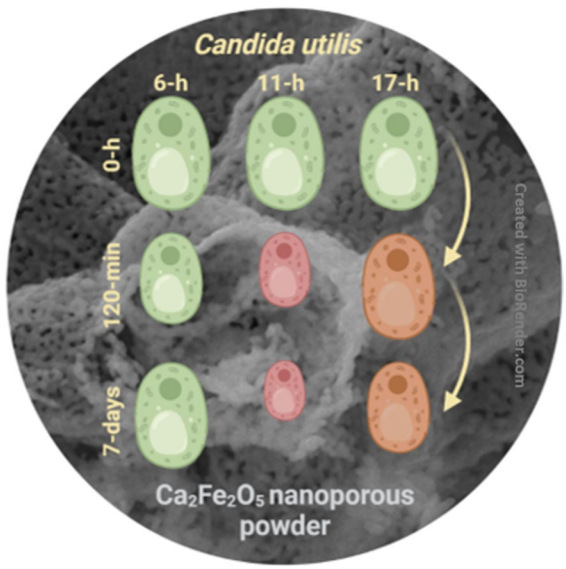

Keywords Antifungal · fungi · Yeast · *Candida utilis* · Ca-Fe oxide · Growth kinetics

Supplementary Information The online version contains supplementary material available at https://doi.org/10.1007/s10534-022-00429-x.

S. Vihodceva (✉) · A. Šutka
The Institute of Materials and Surface Engineering, Faculty of Materials Science and Applied Chemistry, Riga Technical University, 7 Paula Valdena Str, LV-1048 Riga, Latvia
e-mail: Svetlana.Vihodceva@rtu.lv

V. Bankovskis
Biosan Ltd, 7/2 Ratsupites Str, LV-1067 Riga, Latvia

O. Muter
Department of Microbiology and Biotechnology, Faculty of Biology, University of Latvia, 1 Jelgavas Str, LV- 1004 Riga, Latvia

Introduction

Fungal infections represent a global health problem, due to the health risk and conventional drug resistance, especially for immunocompromised patients (Wisplinghoff et al. 2004; Coad et al. 2014; Shivadasan et al. 2016; Abdelhamid et al. 2016, 2020; Mishra et al. 2021). *Candida* species are the most common fungi isolates that cause nosocomial infections (e.g., hospital-acquired infections) (Mukherjee et al. 2004; Wisplinghoff et al. 2004; Abdelhamid et al. 2016; Mishra et al. 2021). Nowadays, rare fungal species of low pathogenic potential, or even species never described as a cause of disease, are being more commonly detected in healthcare settings (Valenza et al. 2006; Cabral et al. 2013). Thus, intensive research and development of novel antifungal agents are of current interest (Coad et al. 2014; Shivadasan et al. 2016; Abdelhamid et al. 2016, 2020, 2021; Mishra et al. 2021). *Candida utilis* yeast (i.e., unicellular fungi reproducing by budding or fission (Russell et al. 2003; Buerth et al. 2011) is an anamorphic form of *Pichia jadinii*, known for its industrial applications and is generally classified as generally recognized as safe (GRAS) by regulatory authorities and rarely associated with the disease (Hazen et al. 1999; Buerth et al. 2011; Scoppettuolo et al. 2014; Watanasrisin et al. 2016; Krahulec et al. 2020). Although, cases of the fungemia, bloodstream, urinary tract, and ocular infections (Hazen et al. 1999; Lukic-Grlić et al. 2011; Scoppettuolo et al. 2014; Shivadasan et al. 2016; Watanasrisin et al. 2016) caused by this yeast (a type of fungus) in humans have been reported among different fungal pathogens. Recently, there has been a growing interest in applying metal and metal oxide-based agents against *Candida* species (Table 1).

One of the most important factors influencing the fungus' resistance to antimicrobials is the phase of growth. Extreme resistance of *Candida glabrata* to oxidative stress has been shown for stationary-phase cells. It was suggested that stress-related transcription factors Yap1p, Skn7p, and Msn4p (Cuéllar-Cruz et al. 2008) were played the main role in this effect. Yet, stationary phase *Candida albicans* yeast cells show properties of better adherence, virulence, and elevated drug resistance. This phenomenon was explained by the fact that many *C. albicans* genes associated with virulence, drug resistance, and cell-wall biosynthesis were expressed only at the stationary phase (Uppuluri et al. 2007). Another study reported that the *C. albicans* culture at the stationary phase regulates the oxidative stress by releasing protective molecules into the surrounding medium. At the same time, oxidative stress would commonly kill actively growing cells (Westwater et al. 2005). The microscopic observation of *C. albicans* cells in the assay with propidium iodide showed that batch cultures became more resistant to the action of chlorhexidine during the transition from exponential growth to the early stationary phase (Suci et al. 2003). At the late stationary phase, *C. utilis* cells appear to become more adaptive to environmental stress (Roy et al. 1998). In the study with *C. utilis*, among 37 identified proteins, 17 proteins were exclusively present in the stationary phase, whereas 3 proteins were specific to the exponential growth phase (Buerth et al. 2011).

Table 1 Summary of some available metal and metal oxide-based agents active against *Candida* species

No.	Material	Organisms	Concentration	Efficiency	References
1	CeMOF	*C. albicans*	40 μg mL^{-1}	93.3%	Abdelhamid et al. (2020)
2	ZnO-chitosan nanocomposite	*C. albicans*	300 μg mL^{-1}	90%	Dananjaya et al. (2018)
3	Al_2O_3 NPs[a]	*C. albicans*, *C. dubliniensis*, *C. glabrata*, *C. tropicalis*, *C. parapsilosis*	766.6 ± 205.4–1866.6 ± 188.5	MFC[a]	Jalal et al. (2016)
4	Nano CuO embedded in polyol-polyester matrix	*C. albicans, C. tropicalis, C. glabrata, C. krusei*	100–1300 μg mL^{-1}	MIC_{90}[a]	Sharmin et al. (2017)
6	Ni-doped ZnO NPs	*C. albicans*	400 μg mL^{-1}	100%	Kumar et al. (2016)
7	$Ag@Fe_2O_3$	*C. albicans*	60 μg mL^{-1}	MIC[a]	Kulkarni et al. (2017)

[a]MFC- minimum fungicidal concentration, MIC-minimum inhibitory concentration

Many materials have been studied and tested for use in antimicrobial applications. Antimicrobial activity has been reported for various metal and metal oxide-based agents. Calcium ferrite $Ca_2Fe_2O_5$ with brownmillerite crystal structure has received a particular interest in recent years and was applied in catalysis (Hirabayashi et al. 2006; Vanags et al. 2021), photocatalysis (Vanags et al. 2019), thin films (Vanags et al. 2019), and oxygen ionic transportation (Shaula et al. 2013; Sun et al. 2018; Karki et al. 2020). Our recent study demonstrated $Ca_2Fe_2O_5$ to be effective in water disinfection by growth inhibition of Gram-negative bacteria *Escherichia coli* and Gram-positive bacteria *Staphylococcus aureus* (Vanags et al. 2021). Importantly, bacteria and fungi represent two distinct biological domains with substantially different cellular physiology and structure (Coad et al. 2014). Data from the literature indicate that antimicrobial materials that are active against bacteria can show no or low effect on fungi, It has been reported that zinc oxide nanoparticles (NPs) are more toxic to prokaryotic cells than eukaryotic cells (Coad et al. 2014). But silver NPs hadn't significant toxic effects on yeasts compared to bacteria (Dorobantu et al. 2015).

In this study fungicidal effect of $Ca_2Fe_2O_5$ was evaluated. We hypothesized that $Ca_2Fe_2O_5$ porous powder (PP) would exhibit the fungicidal effect on *C. utilis* cells, with the different outcomes on the yeast culture being in various phases of growth. To the best of our knowledge, this is the first study to show the fungicidal activity of $Ca_2Fe_2O_5$ PP to *C. utilis* and the impact of the *C. utilis* phase of growth on the cell susceptibility. In this work, the *C. utilis* was exposed to PP in deionized (DI) water to minimize speciation-related effects on toxicity results (Suppi et al. 2015).

Experimental details

Chemicals and synthesis of $Ca_2Fe_2O_5$ porous powder

Iron (iii) nitrate nonahydrate [$Fe(NO_3)_3 \bullet 9H_2O$, ≥ 98%, Merck], calcium nitrate tetrahydrate [$Ca(NO_3)_2 \bullet 4H_2O$, ≥ 98%, Sigma-Aldrich], citric acid monohydrate ($C_6H_8O_7 \cdot H_2O$, > 99%, Merck), ammonia solution (NH_4OH, 25%, Sigma-Aldrich) were used for the $Ca_2Fe_2O_5$ PP synthesis as purchased without further purification. Sodium chloride (NaCl, ≥ 99%, Centro-Chem), Yeast Extract (Biolife), Tryptone (Biolife), and Agar (Merck) were used for the antifungal tests. DI water was used for the synthesis and antifungal tests.

$Ca_2Fe_2O_5$ PP was synthesized by the sol-gel autocombustion method described in our previous works (Vanags et al. 2019, 2021).

$Ca_2Fe_2O_5$ porous powder characterization and instruments

Crystalline phases and purity of the synthesized PP were analyzed by Rigaku MiniFlex X-ray diffractometer (XRD) with Cu Kα (λ 1.540593 Å) radiation in the scan range 5–90°. The morphology, particle and poresize distribution of synthesized PP were characterized and measured using a scanning electron microscope (SEM, Lyra, Tescan). To examine PP colloidal stability and surface charge, the average hydrodynamic diameter (dh) and zeta (ζ) potential of PP (50 mg L^{-1}) in DI water were measured using Zetasizer Nano ZS (Malvern Instruments, UK).

Yeast strain and cultivation conditions

Candida utilis LMKK45 was obtained from the Microbial Strain Collection of Latvia(MSCL). The *C. utilis* was cultivated in the RTS-1 bioreactor (Biosan Ltd., Latvia), which operates based on the patented Reverse-Spin technology (Fig. S1). The optical density of the culture was measured automatically every 20 min at a wavelength of 850 nm, using a near-infrared optical system. The cultures were grown aerobically in 50 mL CORNING® mini-bioreactor tubes (NY, 14,831, Mexico) with a vented cup containing 10 mL of yeast extract peptone dextrose (YPD) broth (containing per L: peptone – 20 g; yeast extract – 10 g; dextrose – 20 g), with the agitation speed of 250 rpm, reverse spin interval of 2 s, at 30 °C. Biomass was harvested after 6 h, 11 h, and 17 h of cultivation. Afterwards, cells were washed by centrifugation at 10,000 rpm for 5 min and resuspended in sterile DI water with the final cells concentration of 10^5 colony forming units (CFU) mL^{-1}. More additional information and experiment visualization (Fig. S1) is found in the Supplementary Material (SM). Each experiment was performed at least in triplicate. Stock suspensions of $Ca_2Fe_2O_5$ PP were prepared in

DI water without ultrasonication and before fungicidal testing, were vigorously vortexed.

The K_{max} was calculated by plotting OD_{850}/(time) data into ln(OD_{850})/time graph. Maximal linear slope of [ln(OD_{850})/(time)] curve is equal to the maximal growth rate and denoted as K(max)(1/h). Doubling time corresponds to ln2/K. Other data outside K_{max} site of [ln(OD_{850})]/(time) curve represents the growth rate and is named K(1/h) [Eq. (1)].

$$K\left(\frac{1}{hr}\right) = \ln\left(\frac{OD_{850}(n)}{OD_{850}(n-1)}\right)/(t(n) - t(n-1)) \quad (1)$$

where K—growth rate; (n) and (n − 1)—time interval.

In vitro Testing of fungicidal activity

Testing was performed in a 96-well microplate with 150 µL cell suspension and 150 µL $Ca_2Fe_2O_5$ PP (1 g L^{-1} in DI water) per well. The control (non-exposed) set contained 150 µL cell suspension and 150 µL DI. All variants were performed in triplicate. The microplate was incubated at 23 °C for 24 h without shaking in the dark. Cell viability was assessed by plating, making decimal dilutions in DI from 10^{-1} to 10^{-5}. The cell suspension was plated onto solidified YPD medium. The CFU were counted after 24 h incubation at 30 °C. Log reduction was calculated using the following equation [Eq. (2)]:

$$Log\ reduction = log_{10}\left(\frac{N_0}{N}\right) \quad (2)$$

where N_0 and N are the numbers of CFU before and after treatment.

Microscopic examination of yeast cells by light microscopy

The analysis of samples preparations and measurements of the lengths of 100 randomly selected *C. utilis* cells were carried out under the light microscope Motic (China), using 100x oil-immersion objective lens and Motic Images Plus 2.0ML software.

Statistical analysis

The cultivation experiments and antifungal tests were performed in triplicate. The data presented in the figures have been expressed as the mean value ± standard deviation. The differences between the treatments were assessed by the Student's *t*-test and one-way analysis of variance (one-way ANOVA) in Microsoft Excel and Office365.

Results

$Ca_2Fe_2O_5$ porous powder characterization

The morphologyof the $Ca_2Fe_2O_5$ PP was studied using SEM (Fig. 1A–D), the particle and pore size distribution was estimated by measuring the diameter of 100 pores (Fig. 1E) and particles (grains) (Fig. 1F). A particle size distribution histogram determined from the SEM images shows a considerable variation in the size, with an average particle length of ~ 129 nm (Fig. 1F). The hydrodynamic diameter of $Ca_2Fe_2O_5$ PP in DI water (0 h) was 3364.5 ± 76 nm with a polydispersity index (PdI) of 0.47 and ζ-potential (0 h) – 6.54 ± 1.94 mV, which means the formed highly polydisperse colloidal system is quite unstable (Ardani et al. 2017). However, there were not observed significant ζ-potential changes after 120 min – 8.06 ± 4.74 mV of PP incubation in DI water compared with as-prepared (0 h) samples. Stock suspensions pH ~ 7.5 visualization (Fig. S2) is in the SM.

The XRD studies showed the formation of a phase-pure $Ca_2Fe_2O_5$ belonging to the brownmillerite group (database code ICDD 00-047-1744) after annealing at 800 °C for 20 min (Fig. 2). Its structure consists of iron oxide octahedra and tetrahedra where calcium ions are located at the interstitial sites. (Sun et al. 2018; Vanags et al. 2021)

Growth kinetics of *Candida utilis*

The culture of *C. utilis* has been harvested after 6 h, 11 h, and 17 h of cultivation, which corresponded to different stages of the culture growth. The shape of a growth curve of the *C. utilis* culture is presented in Fig. 3A. The growth rate expressed as (ΔOD_{850}/Δt) was equal at the 6th and 17th hour (0.11), while at the 11th, the value achieved 0.61 (Fig. 3B). Two linear parts on the plot of lnOD_{850} were determined at time intervals from [5.37 to 7.05 h] and from [7.05 to 10.07 h], with $R^2 = 0.9974$ and $R^2 = 0.9991$,

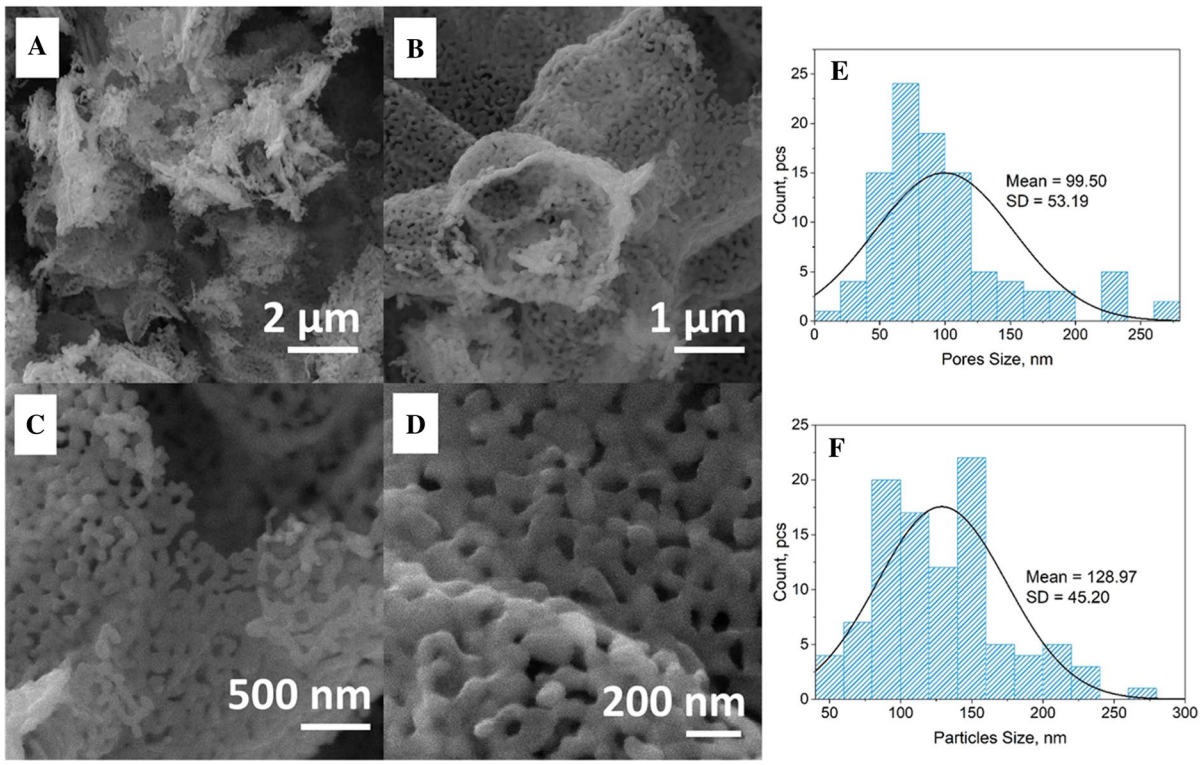

Fig. 1 SEM images (**A**–**D**) of $Ca_2Fe_2O_5$ porous powder at different magnifications. The size distribution histograms, with normal distribution curves, show: **E** pore size distribution; **F** particle size distribution. The mean value and standard deviation (SD) are reported

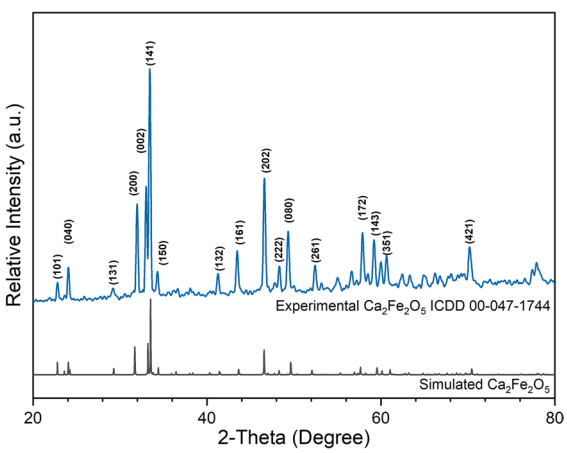

Fig. 2 X-ray diffraction pattern of $Ca_2Fe_2O_5$ PP annealed at 800 °C for 20 min (database code ICDD 00-047-1744)

respectively (Fig. 3C, D). The trendline in a time interval from [5.37 to 10.07 h] also showed a quite high $R^2 = 0.9909$. However, a more precise determination of linear intervals during the exponential phase of growth (as shown in Fig. 3C, D), probably, indicated to the diauxic growth, when at 7.05 h ($OD_{850} = 0.43$) the maximal growth rate has changed from $K = 0.72\ h^{-1}$ to $K = 0.45\ h^{-1}$. This effect can be caused by substrate limitation in YPD broth (e.g., O_2 or L-serine). The values of K for 6 h, 11 h, and 17 h cultures were 0.88 h^{-1}, 0.36 h^{-1}, and 0.02 h^{-1}, respectively. The doubling time for these cultures was found to be 0.79 h, 1.91 h, and 37.30 h, respectively.

Effect of $Ca_2Fe_2O_5$ on the log reduction of *Candida utilis* cells

The log reduction of *C. utilis* in the presence of a $Ca_2Fe_2O_5$ PP is shown in Fig. 4. Thus, for 11 and 17 h old cultures, the trend of CFU reduction was similar and gradually increased with time from 0.34 to 0.87 after 15 min up to 4.22 and 4.10 log—after 7 days' exposition, respectively. It was also evident that the most resistant cells to $Ca_2Fe_2O_5$ PP were detected

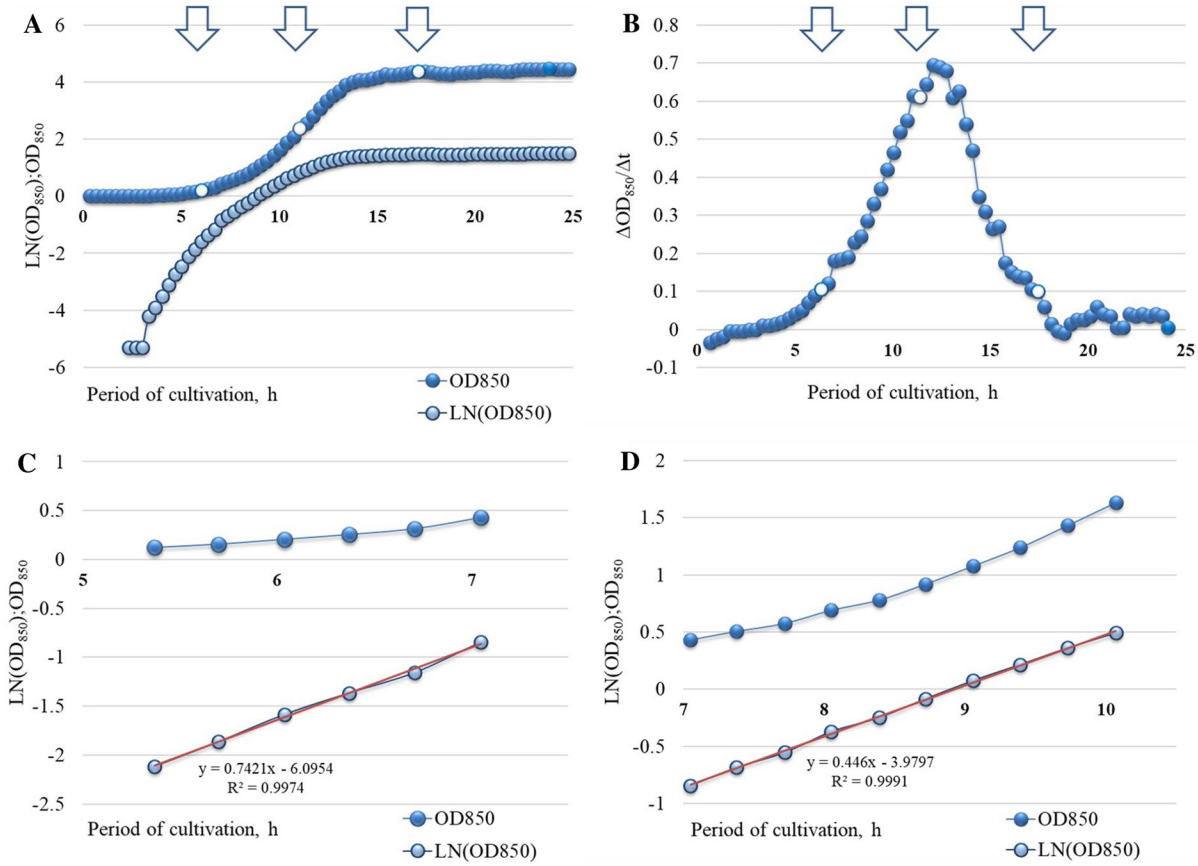

Fig. 3 Growth kinetics of the *Candida utilis* culture. **A** growth curve; **B** growth rate; **C** and **D** time intervals with the maximum growth rate, determined from the slope of a linear fit function. Colorless markers in the curves and arrows above—sampling time, i.e., 6 h, 11 h, and 17 h

in the 6 hold culture, which exhibited a log reduction of <1.0 for exposition periods from 15 min up to 7 days (Fig. 4).

Changes of the yeast cell length after culture incubation with $Ca_2Fe_2O_5$

The physiological response of yeast cells to the presence of antimicrobial materials might have resulted in morphological changes. In this respect, the length of cells was measured after 60 min incubation either in DI water (control) and DI with $Ca_2Fe_2O_5$ to compare the effect of PP on the yeast cells being in different physiological states. Yeast cell preparations are visualized in Fig. 5, while Fig. 6 summarizes the data on cell length measurements. Microscopic examination of the cells showed cell shrinkage for all three tested cultures (i.e., 6 h, 11 h, and 17 h) after 60 min (see Fig. 5D–F) and 7 days (data not shown) in response to $Ca_2Fe_2O_5$ PP. Figure 6 represents the mean lengths of 100 randomly selected yeast cells of *C. utilis* after 60 min and 7 days of cultivation in DI water (control) and DI water with $Ca_2Fe_2O_5$ (1 g L^{-1}). The changes in cell length were statistically significant ($p<0.05$). At the same time, a comparison of cells morphology incubated in DI water, harvested at 6 h, 11 h, and 17 h, did not reveal any statistically significant differences in cells length after 60 min and 7 days. Significant ($p<0.05$) differences were detected between $Ca_2Fe_2O_5$ exposed cells, particularly 6 h- versus 17 h old cultures after 60 min exposition and 6 h- versus 11 h old cultures after 7 days exposition (Fig. 6).

As shown in Fig. 5, preparations of yeast suspensions in the DI water represent the evenly distributed cells (Fig. 5A–C, while preparations with $Ca_2Fe_2O_5$—conglomerates of cells and PP (Fig. 5D–F).

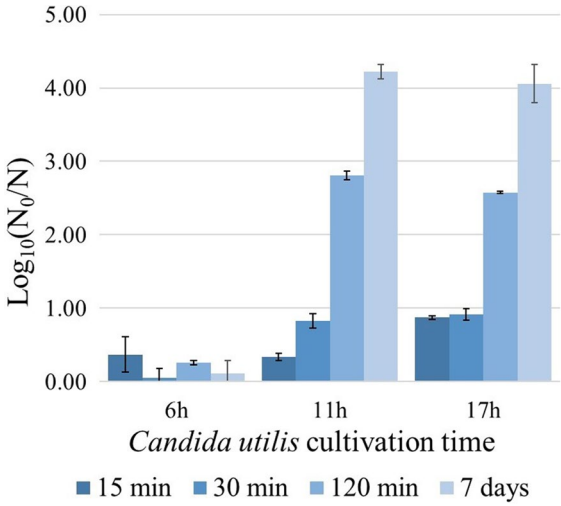

Fig. 4 Mean log reduction of 6 h, 11 h, and 17 h cultivated cells of *Candida utilis* exposed to 1 g L^{-1} $Ca_2Fe_2O_5$ PP compared with controls. Period of cells incubation with $Ca_2Fe_2O_5$—15 min, 30 min, 120 min, and 7 days. The mean value of three repetitions ± standard deviation (SD) is reported. Experiment visualization is in the SM (Fig. S3)

Discussion

According to our previous work, the driving mechanism of $Ca_2Fe_2O_5$ disinfection performance has been identified as the formation of the highly reactive ·OH radicals (ROS) in suspension without light activation—catalysis in the dark. These ·OH radicals are formed due to charge imbalance introduced by the rapid Ca^{2+} leakage from the $Ca_2Fe_2O_5$ structure. The produced radicals can partially or wholly degrade organic contaminants, including microbes (Vanags et al. 2021). It is known that in eukaryotic cells, calcium ions (Ca^{2+}) function as an intracellular signal molecule regulating many different biological processes, including proliferation, muscle contraction, neurotransmitter release, programmed cell death, gene expression, etc. (Cui et al. 2009). Regarding yeast cells, in response to rapid increases in extracellular Ca^{2+}, cytosolic free Ca^{2+} levels rapidly rise and fall with complex dynamics. Due to these changes, the universal Ca^{2+} sensor protein calmodulin can bind and activate the protein phosphatase calcineurin,

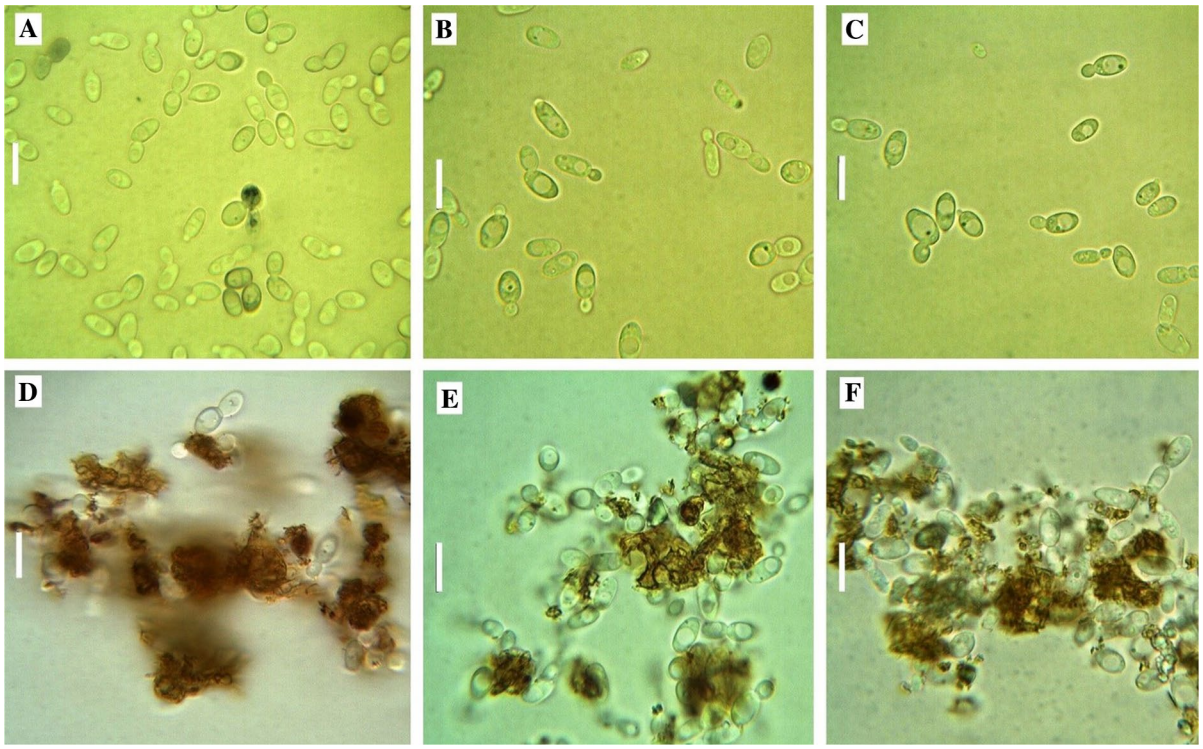

Fig. 5 Light microscopy of *Candida utilis* cells harvested after 6-h (**A**, **D**), 11-h (**B**, **E**), and 17-h (**C**, **F**) cultivation, and cells treated with 1 g L^{-1} $Ca_2Fe_2O_5$ PP for 60 min (**D**–**F**). Bar 10 µm

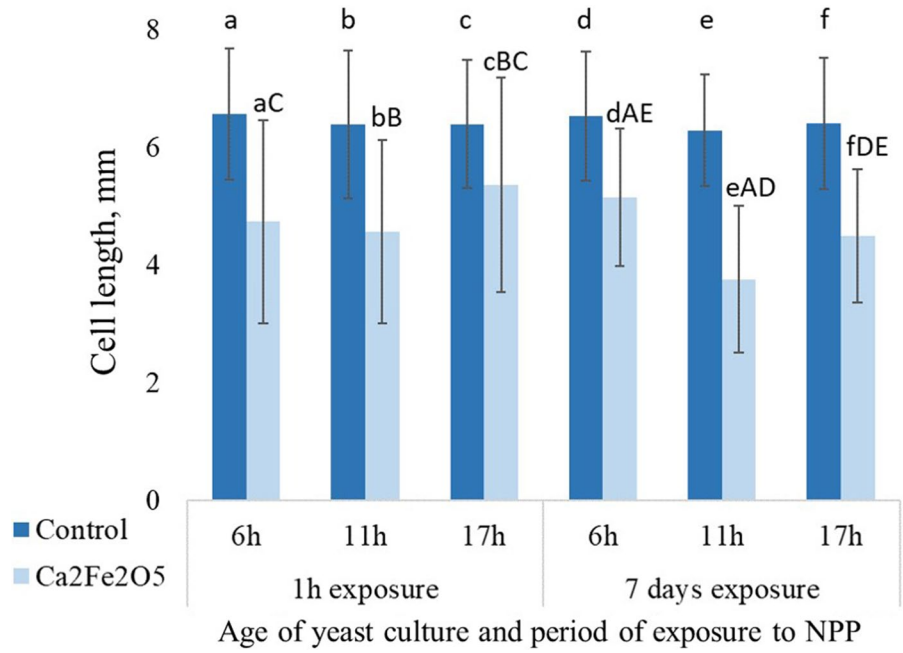

Fig. 6 Mean length of cells in the cultures of *Candida utilis*, harvested after 6 h, 11 h, and 17 h cultivation. Control—cells in DI water; $Ca_2Fe_2O_5$—cells in DI water with 1 g L^{-1} $Ca_2Fe_2O_5$. Small letters are attributed to a comparison of the control and treated cells, while capital letters - treated cells of different culture age and period of exposition, respectively. The mean value of three repetitions ± SD is reported. Statistically significant ($p < 0.05$) differences are indicated with the same letter

which inhibits the function of Vcx1 and induces the expression of Pmc1 and Pmr1 via activation of the Crz1 transcription factor. These calcineurin-sensitive adaptations appear critical for the proliferation of yeast cells in high-calcium environments (Cui et al. 2009; Chen et al. 2020) reported that the intracellular ROS accumulation in *C. utilis* cells leads to the imbalance of intracellular redox state, the elevation of mitochondrial ROS and cytoplasmic Ca^{2+}, damage of mitochondrial mass, and conversion between the reduced and oxidized cytochrome *c*.

he results presented here show the *C. utilis* cell log reduction in response to $Ca_2Fe_2O_5$ PP, with distinct differences in dependence on the culture cultivation time. The data on the highest resistance to $Ca_2Fe_2O_5$ of the 6 h culture of *C. utilis*, compared with 11 and 17 h cultures, -do not corroborate with a recently existing concept. Specifically, it is considered that eukaryotic cells (e.g., yeast) entering the stationary phase are characterized by increased resistance to various environmental stresses. The entry into resting states is typically accompanied by a dramatic decrease in the overall growth rate (Herman et al. 2002). The decrease in metabolic functions of yeast cells at higher cell densities are supposed to be caused by components of the external medium, e.g., carbon dioxide, oxygen, carbon sources, and others (Janda et al. 1985; Ordaz et al. 2001; Tobajas et al. 2003). Besides, the growth kinetics and physiological state of the *C. utilis* culture are dependent on the physical parameters of cultivation, and the physiological state of the inoculum (Šestáková et al. 1979). The growth kinetic parameters for the batch culture of *C. utilis* were determined by Tobajas and Garcia-Calvo (2000). Thus, the Kmax of *C. utilis* in a mineral medium varied from 0.37 h^{-1} to 0.49 h^{-1} at initial glucose concentrations of 7.9 g L^{-1} and 8.6 g L^{-1}, respectively (Tobajas et al. 2000). The earlier studies of batch cultures of *C. utilis*, which were grown with tuna juice-derived sugars, also showed the dependence of Kmax on the initial concentration of sugars (0.39 h^{-1} and 0.47 h^{-1} at sugar concentrations of 33.48 g L^{-1} and 10.77 g L^{-1}, respectively (Paredes Lopez et al. 1976). Analysis of growth kinetics in our study showed two linear intervals within the exponential phase, where at 7.05 h ($OD_{850} = 0.43$), the maximal growth rate has changed from $K = 0.72$ h^{-1} to $K = 0.45$ h^{-1} (Fig. 3C, D). Most probably, the culture harvested after 7.05 h would exhibit a lower resistance towards $Ca_2Fe_2O_5$ than the 6 h culture. However, this hypothesis needs to be checked in further experiments. In our experiments, the Kmax was considerably higher than that reported for *C. utilis* in the batch culture (Paredes et al. 1976; Tobajas et al. 2000). This effect can be explained by specific cultivation conditions used in this study. First, the broth composition is

crucial in determining the growth kinetics. The YPD broth contains peptone, which makes it rich in nutrients compared to a mineral medium. Second, the cultivation of *C. utilis* in RTS-1 bioreactor can result in different growth kinetics compared with conventional bioreactors, because of a reverse spin during agitation. Third, aeration conditions influence the growth rate. The Corning® mini bioreactor tubes with vented cups were used in our experiments. Yet, the ratio of liquid and air phase 1:4 undoubtedly favored the aeration upon culture growth. All these factors could contribute to the enhanced growth rate. In this respect, further studies on the variability of yeast cell resistance to antimicrobials should focus on the test culture's physiological state. Moreover, not only liquid cultures but also biofilms should be tested. Thus, in the study on *C. albicans*, the cell resistance to azoles was compared for biofilm and planktonic populations of exponentially and stationary-phase cultures. The higher resistance was shown for biofilms, where a subpopulation of highly tolerant cells ("persisters", which are not mutants but phenotypic variants of the wild type) can survive at killing doses of antimicrobials and re-growth (LaFleur et al. 2006).

Changes in the cell size upon culture incubation with $Ca_2Fe_2O_5$ PP can be evidence of the stress conditions. Other authors have already reported the changes in yeast cell size, likely to be an indicator of stress conditions. Thus, in the study with *Saccharomyces cerevisiae*, a rapid temperature shift from 33 to 43 °C resulted in an immediate reduction of growth, followed by an increasing subpopulation of significantly smaller cells and loss of viability (Tibayrenc et al. 2010). Lirova et al. (1978) observed that at alkaline pH 7.8 values of the growing medium, the whole cellular organization of *C. utilis* was disordered: the cells were larger, the size of vacuoles increased, and the structure became heterogeneous, but at acid pH values, the cells were smaller than in the control. Nevertheless, the mechanisms of the fungicidal effect of $Ca_2Fe_2O_5$ and other antimicrobials remain poorly understood and need further studies regarding risk assessment and new aspects of yeast physiology.

Conclusion

The $Ca_2Fe_2O_5$ PP exhibited the time-depended fungicidal activity towards *C. utilis* cells for 11 and 17 h cultures. The 6 h culture of *C. utilis* showed enhanced resistance to $Ca_2Fe_2O_5$ PP. Incubation of *C. utilis* cells in the presence of $Ca_2Fe_2O_5$ PP resulted in a significant ($p < 0.05$) decrease of the cell length compared to the control. The most pronounced changes were detected in an 11-h culture after 7 days of incubation, with40% reduction of the cell size and a 4-log reduction of *C. utilis*.

Acknowledgements This work has been supported by the European Regional Development Fund within the Activity 1.1.1.2 "Post-doctoral Research Aid" of the Specific Aid Objective 1.1.1 "To increase the research and innovative capacity of scientific institutions of Latvia and the ability to attract external financing, investing in human resources and infrastructure" of the Operational Programme "Growth and Employment" (No. 1.1.1.2/VIAA/2/18/331). A.Šutka is acknowledging the ERA-NET Cofound, M-era.Net Project CaFeOx No. ES RTD/2021/11.

Declarations

Conflict of interest The authors declare no conflict of interest.

References

Abdelhamid HN, Kumaran S, Wu HW (2016) One-spot synthesis of $CuFeO_2$ nanoparticles capped with glycerol and proteomic analysis of their nanocytotoxicity against fungi. RSC Adv 100:97629–97635. https://doi.org/10.1039/C6RA13396G

Abdelhamid HN, Mahmoud GAE, Sharmouk W (2020) A cerium-based MOFzyme with multi-enzyme-like activity for the disruption and inhibition of fungal recolonization. J Mater Chem B 8:7548–7556

Abdelhamid HN, Mathew AP (2021) Cellulose-Based Materials for Water Remediation: Adsorption, Catalysis, and Antifouling. Front Chem Eng 3:790314. https://doi.org/10.3389/fceng.2021.790314

Ardani HK, Imawan C, Handayani W, Djuhana D, Harmoko A, Fauzia V (2017) Enhancement of the stability of silver nanoparticles synthesized using aqueous extract of *Diospyros discolor* Willd. Leaves using polyvinyl alcohol. IOP Conf Ser 188:012056. https://doi.org/10.1088/1757-899X/188/1/012056

Buerth C, Heilmann CJ, Klis FM, de Koster CG, Ernst JF, Tielker D (2011) Growth-dependent secretome of *Candida utilis*. Microb 157:2493–2503. https://doi.org/10.1099/mic.0.049320-0

Cabral ME, Figueroa LIC, Fariña JI (2013) Synergistic antifungal activity of statin-azole associations as witnessed by *Saccharomyces cerevisiae*- and *Candida utilis*-bioassays and ergosterol quantification. Rev Iberoam Micol 30:31–38. https://doi.org/10.1016/j.riam.2012.09.006

Chen Z, Liu JH, Tian LJ, Zhang Q, Guan Y, Chen L, Liu G, Yu H, Tian Y, Huang Q (2020) Raman micro-spectroscopy monitoring of cytochrome c redox state in *Candida utilis*

under low temperature plasma-induced oxidative stress. Analyst 145:3922–3930. https://doi.org/10.1039/d0an00507j

Coad BR, Kidd SE, Ellis DH, Griesser HJ (2014) Biomaterials surfaces capable of resisting fungal attachment and biofilm formation. Biotechnol Adv 32:296–307. https://doi.org/10.1016/j.biotechadv.2013.10.015

Cui J, Kaandorp JA, Ositelu OO, Beaudry V, Knight A, Nanfack YF, Cunningham KW (2009) Simulating calcium influx and free calcium concentrations in yeast. Cell Calcium 45:123–132. https://doi.org/10.1016/j.ceca.2008.07.005

Cuéllar-Cruz M, Briones-Martin-del-Campo M, Cañas-Villamar I, Montalvo-Arredondo J, Riego-Ruiz L, Castaño I, De Las Peñas A (2008) High resistance to oxidative stress in the fungal pathogen *Candida glabrata* is mediated by a single catalase, Cta1p, and is controlled by the transcription factors Yap1p, Skn7p, Msn2p, and Msn4p. Eukaryot Cell 7:814–825. https://doi.org/10.1128/EC.00011-08374

Dananjaya SHS, Kumar RS, Yang M, Nikapitiya C, Lee J, De Zoysa M (2018) Synthesis, characterization of ZnO-chitosan nanocomposites and evaluation of its antifungal activity against pathogenic *Candida albicans*. Int J Biol Macromol 108:1281–1288. https://doi.org/10.1016/j.ijbiomac.2017.11.04

Dorobantu LS, Fallone C, Noble AJ, Veinot J, Ma G, Goss GG, Burrell RE (2015) Toxicity of silver nanoparticles against bacteria, yeast, and algae. J Nanoparticle Res 17:172. https://doi.org/10.1007/s11051-015-2984-7

Hazen KC, Gordon WT, Howell SA (1999) Chronic urinary tract infection due to *Candida utilis*. J Clin Microbiol 37:824–827. https://doi.org/10.1128/JCM.37.3.824-827.1999

Herman PK (2002) Stationary phase in yeast. Curr Opin Microbiol 5:602–607. https://doi.org/10.1016/S1369-5274(02)00377-6

Hirabayashi D, Yoshikawa T, Mochizuki K, Suzuki K, Sakai Y (2006) Formation of brownmillerite type calcium ferrite (Ca2Fe2O5) and catalytic properties in propylene combustion. Catal Lett 110:269–274. doi:https://doi.org/10.1007/s10562-006-0120-0

Jalal M, Ansari MA, Shukla AK, Ali SG, Khan HM, Pal R, Alam J, Cameotra SS (2016) Green synthesis and antifungal activity of Al_2O_3 NPs against fluconazole-resistant *Candida* spp isolated from a tertiary care hospital. RSC Adv 6:107577–107590. https://doi.org/10.1039/c6ra23365a

Janda S, Kotyk A (1985) Effects of suspension density on microbial metabolic processes. Folia Microbiol 30:465–473. https://doi.org/10.1007/BF02927608

Karki SB, Hona RK, Ramezanipour F (2020) Effect of structure on sensor properties of oxygen deficient perovskites, A2BB′O5 (A = Ca, Sr; B = Fe; B′ = Fe, Mn) for oxygen, carbon dioxide and carbon monoxide sensing. J Electron Mater 49:1557–1567. https://doi.org/10.1007/s11664-019-07862-8

Krahulec J, Lišková V, Boňková H, Lichvariková A, Šafranek M, Turňa J (2020) The ploidydetermination of the biotechnologically important yeast *Candida utilis*. J Appl Genetics 61:275–286. https://doi.org/10.1007/s13353-020-00544-w

Kulkarni S, Jadhav M, Raikar P, Barretto DA, Vootla SK, Raikar US (2017) Green synthesized multifunctional Ag@Fe_2O_3 nanocomposites for effective antibacterial, antifungal and anticancer properties. New J Chem 41:9513–9520. doi:https://doi.org/10.1039/c7nj01849e

Kumar RS, Dananjaya SHS, De Zoysa M, Yang M (2016) Enhanced antifungal activity of Ni-doped ZnO nanostructures under dark conditions. RSC Adv 6:108468–108476. https://doi.org/10.1039/c6ra18442a

LaFleur MD, Kumamoto CA, Lewis K (2006) Candida albicans biofilms produce antifungal-tolerant persister cells. Antimicrob Agents Chemother 50:3839–3846. https://doi.org/10.1128/AAC.00684-06

Lirova SA, Schumann E, Schtrunk K, Khovrychev MP, Rabotnova IL (1978) Effect of pH values of the medium unfavorable for growth on the physiological, morphological and cytological characteristics of a chemostat culture of *Candida utilis*. Microbiologiia 47:414–423

Lukic-Grlić A, Mlinarić-Missoni E, Škaric I, Važic-Babić V, Svetec IK (2011) *Candida utilis* candidaemia in neonatal patients. J Med Microbiol 60:838–841. https://doi.org/10.1099/jmm.0.023408-0

Mishra P, Gupta P, Pruthi V (2021) Cinnamaldehyde incorporated gellan/PVA electrospun nanofibers for eradicating *Candida* biofilm. Mater Sci Eng C 119:111450. https://doi.org/10.1016/j.msec.2020.111450

Mukherjee PK, Chandra J (2004) Candida biofilm resistance. Drug Resist Updates 7:301–309. https://doi.org/10.1016/j.drup.2004.09.002

Ordaz L, López R, Melchy O, De la Torre M (2001) Effect of high-cell-density fermentation of *Candida utilis* on kinetic parameters and the shift to respiro-fermentative metabolism. Appl Microbiol Biotechnol 57:374–378. https://doi.org/10.1007/s002530100677

Paredes Lopez O, Camargo Rubio E, Ornelas Vale A (1976) Influence of specific growth rate on biomass yield, productivity, and composition of *Candida utilis* in batch and continuous culture. Appl Environ Microbiol 31:4. https://doi.org/10.1128/aem.31.4.487-491.1976

Roy A, Ghosh AK (1998) Correlation between stationary phase survival and acid trehalase activity in yeast. Biochim Biophys Acta 1401:235–238. https://doi.org/10.1016/S0167-4889(97)00156-0

Russell AD (2003) Similarities and differencies in the responses of microorganisms to biocides. J Antim Chemother 52:750–763. https://doi.org/10.1093/jac/dkg422

Scoppettuolo G, Donato C, De Carolis E, Vella A, Vaccaro L, La Greca A, Fantoni M (2014) Candida utilis catheter-related bloodstream infection. Med Mycol Case Rep 6:70–72. https://doi.org/10.1016/j.mmcr.2014.10.003

Šestáková M (1979) Growth of *Candida utilis* on a mixture of monosaccharides, acetic acid and ethanol as a model of waste sulphite liquor. Folia Microbiol 24:318–327. https://doi.org/10.1007/BF02926651

Sharmin E, Shreaz S, Zafar F, Akram D, Raja V, Ahmad S (2017) Linseed polyol-assisted, microwave-induced synthesis of nano CuO embedded in polyol-polyester matrix: antifungal behavior and coating properties. Prog Org Coat 105:200–211. https://doi.org/10.1016/j.porgcoat.2017.01.001

Shaula AL, Kolotygin VA, Naumovich EN, Pivak YV, Kharton VV (2013) Oxygen ionic transport in brownmillerite-type Ca2Fe2O5-δ and calcium ferrite-based composite membranes. Solid State Phenom 200:286–292

Shivadasan J, Raksha K, Urs PS (2016) *Candida utilis* causing neonatal Candidemia—a case report and literature review. Apollo Med 13:55–58. https://doi.org/10.1016/j.apme.2016.01.001

Suci PA, Tyler BJ (2003) A method for discrimination of subpopulations of *Candida albicans* biofilm cells that exhibit relative levels of phenotypic resistance to chlorhexidine. J Microbiol Methods 53:313–325. https://doi.org/10.1016/S0167-7012(02)00247-6

Sun Z, Chen S, Hu J, Chen A, Rony AH, Russell CK, Xiang W, Fan M, Diar DM, Dklute EC (2018) Ca2Fe2O5: A promising oxygen carrier for CO/CH4 conversion and almost-pure H2 production with inherent CO2 capture over a two-step chemical looping hydrogen generation process. Appl Energy 211:431–442. https://doi.org/10.1016/j.apenergy.2017.11.005

Suppi S, Kasemets K, Ivask A, Künnis-Beres K, Sihtmäe M, Kurvet I, Aruoja V, Kahru A (2015) A novel method for comparison of biocidal properties of nanomaterials to bacteria, yeasts and algae. J Hazard Mater 286:75–84. doi:https://doi.org/10.1016/j.jhazmat.2014.12.027

Tibayrenc P, Preziosi-Belloy L, Roger JM, Ghommidh C (2010) Assessing yeast viability from cell size measurements? J Biotechnol 149:74–80. https://doi.org/10.1016/j.jbiotec.2010.06.019

Tobajas M, Garcia-Calvo E (2000) Comparison of analysis methods for determination of the kinetic parameters in batch cultures. World J Microbiol Biotechnol 16:845–851. https://doi.org/10.1023/A:1008971708358

Tobajas M, García-Calvo E, Wu X, Merchuk JC (2003) A simple mathematical model of the process of *Candida utilis* growth in a bioreactor. World J Microbiol Biotechnol 19:391–398. https://doi.org/10.1023/A:1023942602041

Uppuluri P, Chaffin WLJ (2007) Defining *Candida albicans* stationary phase by cellular and DNA replication, gene expression and regulation. Mol Microbiol 64:1572–1586. https://doi.org/10.1111/j.1365-2958.2007.05760.x

Valenza G, Valenza R, Brederlau J, Frosch M, Kurzai O (2006) Identification of *Candida fabianii* as a cause of lethal septicaemia. Mycoses 49:331–334. https://doi.org/10.1111/j.1439-3420507.2006.01240.x343

Vanags M, Mežule L, Spule A, Kostjukovs J, Šmits K, Tamm A, Juhna T, Vihodceva S, Kaambre T, Baumane L, Začs D, Vasiliev G, Turks M, Mierina I, Sherrell P, Šutka A (2021) Rapid catalytic water disinfection from earth abundant $Ca_2Fe_2O_5$ brownmillerite. Adv Sustain Syst. https://doi.org/10.1002/adsu.202100130

Vanags M, Spule A, Gruškeviča K, Vihodceva S, Tamm A, Vlassov S, Šutka A (2019) Sol-gel auto combustion synthesis of $Ca_2Fe_2O_5$ brownmillerite nanopowders and thin films for advanced oxidation photoelectrochemical water treatment in visible light. J Environ Chem Eng 7:103224. https://doi.org/10.1016/j.jece.2019.10322

Watanasrisin W, Iwatani S, Oura T, Tomita Y, Ikushima S, Chindamporn A, Niimi M, Niimi K, Lamping E, Cannon RD, Kajiwara S (2016) Identification and characterization of *Candida utilis* 350 multidrug efflux transporter CuCdr1p. FEMS Yeast Res 16:fow042. https://doi.org/10.1093/femsyr/fow042

Westwater C, Balish E, Schofield DA (2005) Candida albicans-conditioned medium protects yeast cells from oxidative stress: A possible link between quorum sensing and oxidative stress resistance. Eukaryot Cell 4:1654–1661. https://doi.org/10.1128/EC.4.10.1654-1661.2005

Wisplinghoff H, Bischoff T, Tallent SM, Seifert H, Wenzel RP, Edmond MB (2004) Nosocomial bloodstream infections in US hospitals: analysis of 24,179 cases from a prospective nationwide surveillance study. Clin Infect Dis 39:309–317. https://doi.org/10.1086/421946